Available online at www.sciencedirect.com
ScienceDirect
Journal of the European Ceramic Society 30 (2010) 2603–2615
www.elsevier.com/locate/jeurceramsoc

Determination of reversible and irreversible contributions to the polarization and strain response of soft PZT using the partial unloading method

Dayu Zhou, Ruoyu Wang, Marc Kamlah *

Karlsruhe Institute of Technology, Institute for Materials Research II, D-76021 Karlsruhe, Germany

Received 19 February 2010; received in revised form 22 April 2010; accepted 29 April 2010
Available online 31 May 2010

Abstract

Experimental work is aimed at systematically investigating the non-linear ferroelectric and ferroelastic behavior of a commercially available soft lead zirconate titanate (PZT) material. The fast partial unloading method is used to measure the material properties of unpoled soft PZT under pure electric field and of initially pre-poled soft PZT under compressive stress loading. In the first experiment using unpoled PZT, the evolution of piezoelectric constants and dielectric permittivity is determined as a function of electric field. It is found that the piezoelectric constants and dielectric permittivity depend on the electric field history. The results are used to separate the reversible strain and polarization from the irreversible ones caused by domain switching. In the second experiment using initially pre-poled PZT, it is found that the strain response is significantly dependent on the stress loading rate. The elastic moduli and piezoelectric coefficients are evaluated with respect to the compressive stress history. The measured longitudinal and transverse irreversible strains change significantly during both loading and unloading processes. An attempt is made to discuss the use of irreversible strain and irreversible polarization as internal variables for constitutive modeling. This investigation provides valuable information for modeling to predict the performance and for improving the reliability of piezoelectric devices.

Keywords: Piezoelectric and dielectric hysteresis; Elastic compliance; Irreversible strain; Irreversible polarization; Domain switching

1. Introduction

As one of the main candidates for intelligent materials, ferroelectric piezoceramics are being used increasingly for actuators and sensors in a wide variety of electromechanical applications, including noise controls, active vibration suppression, ultra-high precision positioning, and especially fuel injection valves in new-generation common rail diesel and gasoline engines.[1–4] In practice these devices are subject to severe loading conditions and have complicated geometries which may give rise to local stress or electric field concentration around field intensifiers.[4,5]

The grains of ferroelectric piezoceramics are subdivided into domains separated by domain walls. A domain is a group of unit cells within a grain, all of which have the same spontaneous polarization orientation.[6,7] When applying an appropriate magnitude of an electric field or a mechanical load to a piezoceramic material, the spontaneous polarization direction of domains may be reoriented, which is commonly called ferroelectric or ferroelastic domain switching. It is well known that, when large-signal loads are applied, the responses of piezoceramics exhibit on the macroscale pronounced non-linearity and hysteresis due to the above-mentioned inherent ferroelectric and ferroelastic domain switching and due to consequent changes of the irreversible polarization and strain.[8,9] Macroscopic irreversible polarization and strain are commonly also called "remnant" polarization and strain, respectively. To further assess and improve the reliability of piezoelectric devices, considerable efforts have been made in recent years to develop constitutive models that are capable of accurately predicting the linear behavior and, especially, the non-linear hysteresis behavior, of piezoceramics over a wide range of applied signals.[10,11] The success of constitutive models depends largely on the availability of suitable experimental measurements.

The most frequently encountered loading spectrum is coaxial electromechanical loading. Lynch[8] measured the polarization and strain versus electric field hysteresis loops for (Pb,La)(Zr,Ti)O_3 (PLZT) ceramics at various levels of compression preload (up to −60 MPa). The effects of prestress

* Corresponding author. Tel.: +49 7247 82 5860; fax: +49 7247 82 2347.
E-mail address: marc.kamlah@kit.edu (M. Kamlah).

0955-2219/$ – see front matter © 2010 Elsevier Ltd. All rights reserved.
doi:10.1016/j.jeurceramsoc.2010.04.042

on the remnant polarization, coercive field, and piezoelectric coefficients were studied qualitatively. Chaplya and Carman[9] attributed the non-linear electromechanical response of PZT-5H soft piezoceramics to non-180° domain wall motion processes. Apart from the bipolar ferroelectric hysteresis loops, the polarization and strain responses to a unipolar electric field load were evaluated experimentally at various prestresses (up to −175 MPa). Doing this, larger polarization and strain outputs were observed upon the application of a small compressive preload. Zhou et al.[12] discussed the influence of preload stress on the ferroelectric hysteretic behavior of soft lead zirconate titanate (PZT) piezoceramic material. The polarization and strain versus electric field hysteresis loops were measured under various uniaxial compressive stress preloads (up to −400 MPa). It is revealed that preload stress reduced the remnant polarization, decreased the coercive field, had impact on the material properties, and prevented full alignment of the domains and induced mechanical depolarization. These results could be explained in terms of the non-180° domain switching process. Liu and Huber[13] measured material properties of a soft ferroelectric ceramic under combined loading of uniaxial compressive stress and electric field. The remnant quantities were treated as state variables to express the moduli as functions of the material state. A simple model of the state dependence of the moduli was used to explain the results.

The influence of a DC bias field on the non-linear ferroelastic behavior of piezoceramics had been investigated by several research groups. In the work of Schaeufele and Haerdtl[14] addressed to PZT ceramics with variable Zr:Ti ratios and additive dopants, an electric field applied parallel to the poling direction was found to linearly increase the coercive stress of ferroelastic switching. Chaplya and Carman[15] measured the ferroelastic properties of PZT ceramics under a constant bias electric field, the focus lying on vibration damping applications. Only the stress–strain behavior was evaluated in this work. The observed phenomena were qualitatively explained by non-180° domain wall motion. Application of a parallel bias field resulted in closed stress–strain hysteresis loops and increasing coercive stress. The coercive stress was found to approach zero when an anti-parallel bias field approaching the coercive field value was applied. A linear dependence of the coercive stress on a bias electric field was reported by Zhou et al.[16] in the study of non-linear ferroelastic behavior of soft PZT. Both, stress–depolarization and stress–strain properties were measured systematically over a wide range of superposed constant electric fields.

Several experimental attempts have been made to provide insight into the loading history dependence of material parameters of piezoceramics. Fett et al.[17] studied the change of Young's modulus under compressive stress loading for initially unpoled and pre-poled soft PZT material using the partial unloading method. An increase of Young's modulus was observed with increasing compression load and this effect was found to depend on the poling state of the material. The experimental results were interpreted in terms of combined contributions of lattice deformation and domain wall motion to the linear response. Recently, Selten et al.[18] reported a detailed experimental study of unpoled soft PZT material. Apart from the determination of Young's modulus under cyclic bipolar and unipolar mechanical loads, the changes of dielectric permittivity and piezoelectric constant were measured for the material during the poling process. Time-dependent effects were considered in the design of their measurements.

It is our objective to systematically investigate the non-linear ferroelectric and ferroelastic behavior of a commercially available soft lead zirconate titanate (PZT) material. Special emphasis will be put on distinguishing between reversible and irreversible processes. While reversible contributions in ferroelectrics are due to ionic and electronic displacements and to domain wall motions with a small amplitude, irreversible processes are due to interaction of lattice defects and domain walls as well as nucleation and growth of new domains.[19] The fast small-electric-field and small-stress partial unloading method which could minimize the time-dependent irreversible effects shall be used to measure the material properties of unpoled soft PZT under pure electric field and of initially pre-poled soft PZT under compressive stress loading.[5]

2. Experimental procedures

2.1. Material and specimen preparation

The measurements were performed using PIC151 piezoceramics (PI Ceramic, Lederhose, Germany). This material is a type of $Pb(Ni_{1/3}Sb_{2/3})O_3$–$PbTiO_3$–$PbZrO_3$ ternary phase system formed in the vicinity of the morphotropic phase boundary of PZT in the tetragonal range. A Sb^{5+} dopant acts as a donor to make the material a "soft" PZT. Detailed physical properties of this material can be found on the internet: www.piceramic.de. The specimens were cut and grounded to dimensions 5 mm × 5 mm × 15 mm by the manufacturer. The large aspect ratio of 3:1 can effectively eliminate the clamping effects, in the sense that a uniform uniaxial stress and strain state may be ensured in a large middle portion of the sample.

Following stringent cleaning, four strain gauges were attached to the sample using an M-bond 600 adhesive (Vishay Measurements Group). A pair of strain gauges was fixed to opposite sides to measure the longitudinal strain; another pair was used for monitoring the transverse strain.

To reduce the probability of arcing and obtain correct strain measurements during electric field loading, a thin layer of Kapton polyamide film was placed between the strain gauges and the specimen.

2.2. Experimental set-up

As shown in Fig. 1, a special experimental set-up was built for combined electrical and mechanical tests. A polymer material container was installed on the servohydraulic test frame (model 1361, Instron, Canton, MA). During the experiments, the container was filled with fluorinert electric liquid (FC-40, 3M, St. Paul, MN) to prevent electric discharge. The prepared specimen was positioned in the center between two alumina ceramic spacers to insulate the test frame from the high voltage.

A high electric field was generated by a bipolar high-voltage power supply (HCB 15-30 000, F.u.G, Rosenheim, Germany) and applied to the specimen via the copper shims attached to the alumina blocks. The maximum output of the power supply was ±30 kV which corresponds to ±2 kV/mm on the specimen. The Instron servohydraulic loading frame was used to apply a uniaxial compressive stress to the specimen. A ball-joint assembly was used to minimize bending effects. The Sawyer-Tower method was applied to measure electric polarization. By means of a high-input-resistance electrometer (6517A, Keithley Instruments, Cleveland, OH), voltage variation over a 10 μF reference capacitor was monitored, which was connected in series with the specimen. Four carrier frequency amplifiers (KWS 3073 5 kHz, Hottinger Baldwin Messtechnik, Darmstadt, Germany) were used to monitor the strains.

A computer equipped with a data acquisition board and DASYLAB software (Dasytec, Amherst, NH) was used to digitally record the measurement signals and to control at the same time the Instron machine as well as the high-voltage power supply. All equipment output signals were first passed through isolated dc input/output signal conditioning modules (Phoenix Contact, Blomberg, Germany) and then recorded by the computer. The signal conditioning modules were used for a further insulation of the computer from high-voltage discharge. Further details of the specimen preparation method and electric/mechanical test set-up can be found in the PhD thesis of Zhou.[5]

2.3. Measurement procedures

2.3.1. Initially unpoled soft PZT under electric field loading

Under stress-free conditions departing from an initially unpoled state, the specimen was loaded by a ramp-shaped electric field (main electric field loading) in the following form: $0\,\text{kV/mm} \rightarrow +2.0\,\text{kV/mm} \rightarrow 0.0\,\text{kV/mm} \rightarrow -2.0\,\text{kV/mm} \rightarrow 0.0\,\text{kV/mm} \rightarrow +2.0\,\text{kV/mm} \rightarrow 0.0\,\text{kV/mm}$. The loading rate was quite low: 0.002 kV/mm s. The hysteresis loops of polarization as well as strains in axial and transverse directions versus the electric field were monitored simultaneously.

To achieve the piezoelectric and dielectric constants at a pre-determined value of the main electric field history, the electric field was unloaded partly followed by reloading back to that value, both at a fast rate. The magnitude of the partial unloading cycles was fixed as $\Delta E_3 = 0.1\,\text{kV/mm}$. To minimize the effect of time-dependent processes during unloading cycles, a significantly higher rate of 0.1 kV/mm s was chosen. During ramping up the main electric field, unloading cycles were placed at intervals of 0.05 kV/mm in the range of $0.7\,\text{kV/mm} \leq |E| \leq 1.1\,\text{kV/mm}$, in order to record the drastic changes of the material properties near the coercive field. Outside this range, unloading cycles during ramping the main electric field up were chosen at intervals of 0.1 kV/mm. During ramping the main electric field down, unloading cycles were placed at intervals of 0.2 kV/mm. Hence, the overall loading profile is composed of a continuous quasi-static electric field-time pattern superposed by a set of small-field unloading–reloading pulses.

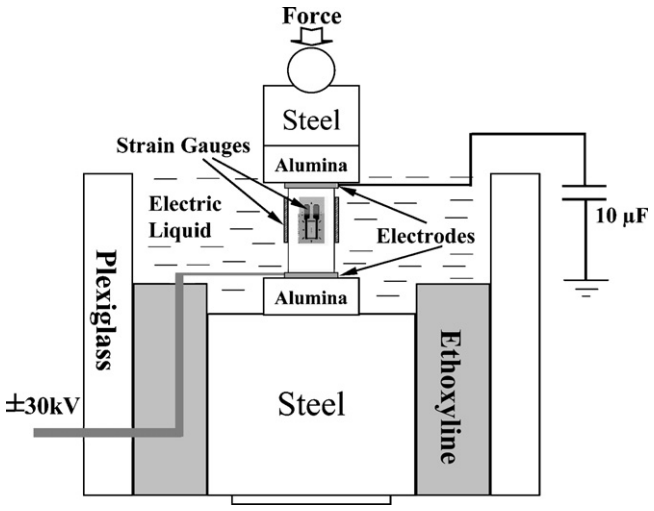

Fig. 1. Experimental set-up.

To ensure the reliability of the experimental results, the measurements were repeated four times using different specimens. The material properties shown below represent the mean value of four measurements.

2.3.2. Pre-poled soft PZT under compressive stress loading

The specimen used for compression tests was first poled by applying an electric field of 1.8 kV/mm for 3 min in the stress-free state. After poling, the material possessed irreversible polarization and irreversible strains. Then, the measurement started and the specimen was subjected to the compression load parallel to the poling direction in the following way: the main compressive stress load was applied in a ramp-shaped waveform from 0.0 MPa to 300.0 MPa and back to 0.0 MPa at a rate of 0.25 MPa/s. Polarization in axial direction as well as longitudinal and transverse strains versus compressive stress were monitored simultaneously.

During both loading and unloading processes the stress was partially unloaded rapidly at pre-determined main stress values, followed by reloading back to this value, to measure the evolution of elastic compliances and piezoelectric constants. The stress magnitude of a partial unloading cycle was set to 10 MPa ($\Delta\sigma_3$), with an unloading–reloading rate of 5 MPa/s. Hence, the overall loading profile consisted of a continuous quasi-static stress–time pattern superposed by a set of small-stress unloading–reloading pulses.

The tests were repeated seven times using different specimens to ensure the reliability of experimental findings. The material parameters shown below represent the mean value of seven measurements.

3. Results and discussion

3.1. Initially unpoled soft PZT under electric field loading

3.1.1. Piezoelectric and dielectric coefficients

Fig. 2 shows the curve of axial strain (S_3) versus electric field (E_3). As described in the previous section, the loading rate of the applied main electric field is very slow ($\dot{E}_3 = 0.002\,\text{kV/(mm s)}$).

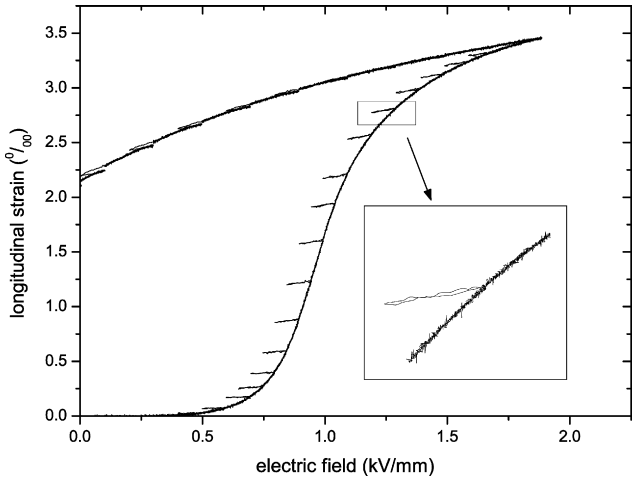

Fig. 2. Electric field–longitudinal strain curve measured by using the partial unloading method.

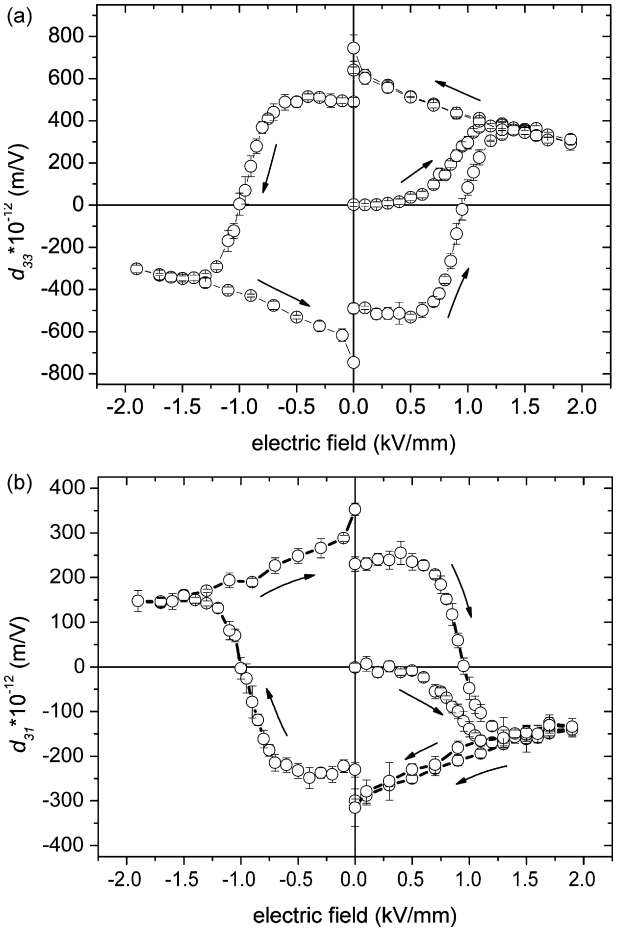

Fig. 3. Piezoelectric constants in axial (a) and transverse (b) directions plotted vs. electric field.

At certain values of the main electric field, partial unloadings were carried out with $\Delta E_3 = 0.1$ kV/mm and $\dot{E}_3 = 0.1$ kV/(mm s). Consequently, the material parameters measured under such conditions correspond to a relatively fixed domain configuration in the sense of a frozen domain state. In other words, the influence of time-dependent effects is minimized.

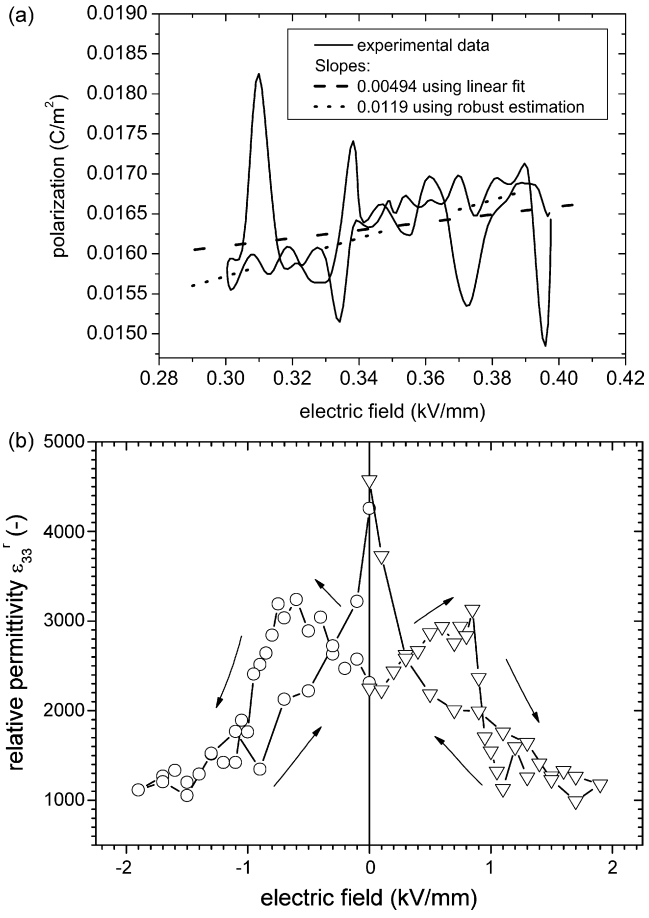

Fig. 4. (a) Comparison of the slopes measured using the robust estimation method and obtained by the linear fit method and (b) relative permittivity in axial direction plotted vs. electric field.

As shown in the inset in Fig. 2, the strain versus electric field curves obtained during the partial unloading period can be fitted well by straight lines. The slopes of the fitting allow the piezoelectric and dielectric constants to be attained at different main field values:

$$d_{33} = \frac{\Delta S_3}{\Delta E_3}, \tag{1}$$

$$d_{31} = \frac{\Delta S_1}{\Delta E_3}, \tag{2}$$

$$\varepsilon_{33} = \frac{\Delta D_3}{\Delta E_3}. \tag{3}$$

Here, ΔS_3 and ΔS_1 are the changes of longitudinal and transverse strains, d_{33} and d_{31} denote the piezoelectric constants in axial and transverse directions, ΔD_3 represents the change of dielectric displacement which is approximately equal to the polarization change ΔP_3, ε_{33} is the dielectric constant, and ΔE_3 stands for the change of the electric field.

As shown in Fig. 3, the piezoelectric constants measured in axial and transverse directions are plotted versus the main electric field at which partial unloading was performed. At first, the initially unpoled macroscopic state is defined to be the state of zero strain ($S = 0$ both in axial and transverse directions). Until

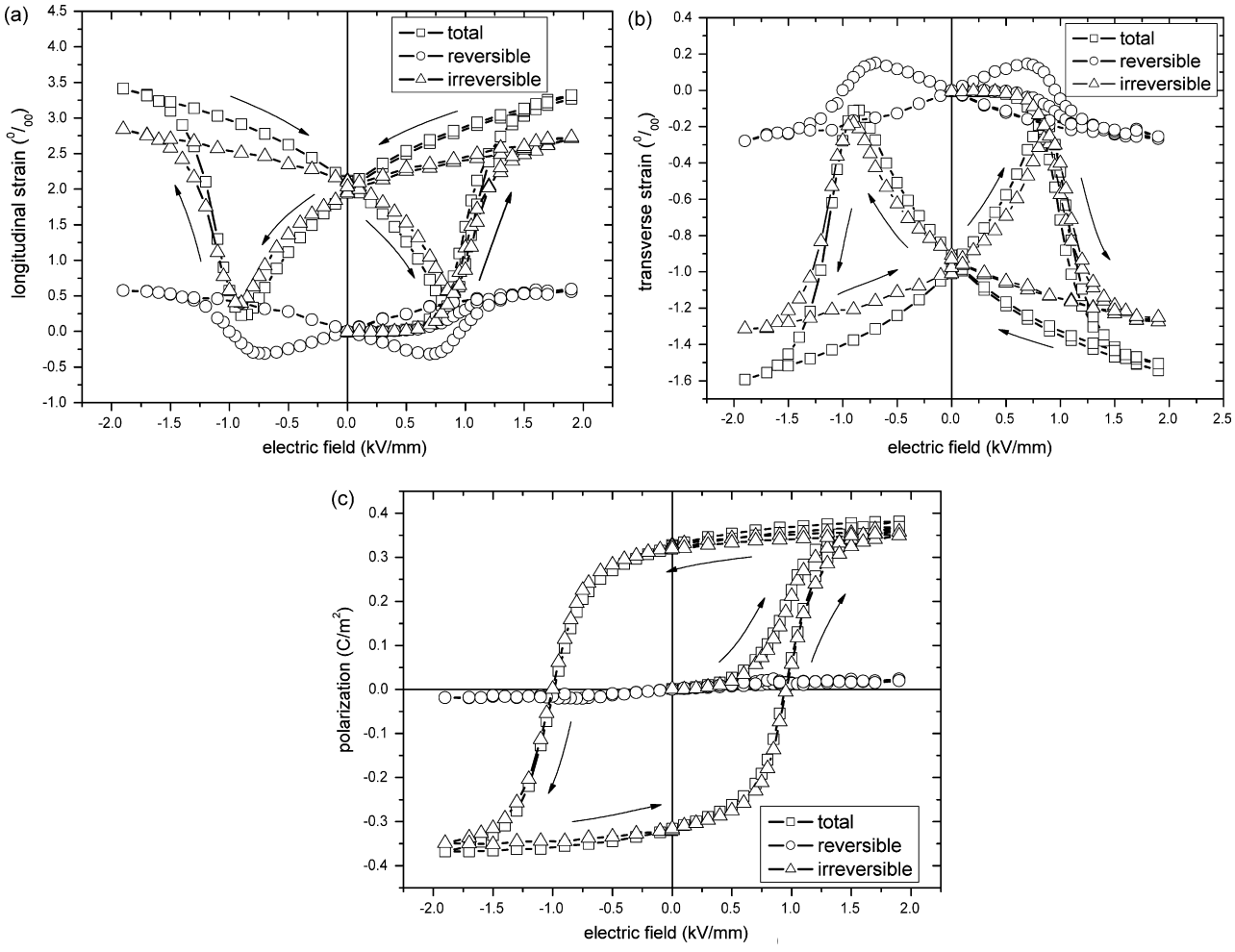

Fig. 5. Total, reversible and irreversible longitudinal (a) and transverse (b) strains and polarization (c) plotted vs. main electric field.

the coercive field is approached, the distribution of the polarization orientation of the domains is random. As a result, the microscopic piezoelectric contributions of the domains cancel each other and no electrically induced macroscopic strains can be observed. Accordingly, the values of the piezoelectric constants versus electric field derived from Eqs. (1) and (2) vanish until the neighborhood of the coercive field is reached.

During the loading process of the electric field in the neighborhood of the coercive field, a significant increase of the magnitudes of both d_{33} and d_{31} is observed. We address this finding to two effects: First, alignment of more and more domains in the direction of the main electric field gives rise to the occurrence and the steady increase of the macroscopic piezoelectric effect. Second, there is a contribution from reversible domain wall motion. This latter assertion is supported by the observation that during unloading cycles in this range, the local hysteresis loops were closed (not shown). It is well known that there are both intrinsic and extrinsic contributions to the piezoelectric response, where the extrinsic contributions are more important in soft PZT.[20,21]

After reaching an intermediate maximum level, the magnitudes of the piezoelectric constants decrease with further increased main electric field. These decreases are presumably related to stronger constraining of the domain walls due to the very high and increasing main electric field. Furthermore, the sample gets closer to a monodomain state where only the intrinsic lattice contributions remain.[22] As the main electric field is reduced, we observe increases of the magnitudes of d_{33} and d_{31}. We suppose this is due to the reduced fixing of domain walls caused by the reduced main electric field. The close to monodomain state is no longer as frozen and there is partial back-switching and more and more extrinsic contribution to the piezoelectric properties.

For technical reasons, the test had to be interrupted each time for a few minutes at zero electric field. A short electric field pulse was applied to the specimen to minimize the negative effect of this hold time but still there occurs some discontinuity in the plots of the piezoelectric constants at zero main electric field. Upon reversing the electric field, the material parameters respond in the same way as before.

To reduce the negative effects of signal noise, the robust estimation method,[23] which fits a line to the data by minimizing the absolute deviation is used instead of the linear fit method for obtaining the dielectric constants in terms of Eq. (3). As shown in Fig. 4(a), the line slope for an unloading cycle obtained using the

robust estimation method is more accurate than the one obtained by the linear fit method.

In Fig. 4(b) the dielectric constant is plotted versus the main electric field. Following common practice, we show the relative permittivity $\varepsilon^r_{33} = \varepsilon_{33}/\varepsilon_0$, where $\varepsilon_0 = 8.85 \times 10^{-12}$ C/(V m) is the vacuum permittivity. The plot shows a clear trend similar to results presented by Böttger.[19] The curve resembles a typical inverse "butterfly" hysteresis loop with two additional humps. The occurrence of two different pairs of humps at $E = \pm 0.7$ kV/mm and $E = \pm 1.1$ kV/mm has been explained by different coercive field strengths for non-180°- and 180°-switching. In the tetragonal phase, the dielectric coefficient takes a minimum at the coercive field strength due to 180°-switching, while 90°-rotation occurs twice, once before and once after reaching the coercive field strength.[24]

3.1.2. Separation of reversible and irreversible strains and polarization

Measurement of material parameters at various electric fields allows for a distinction between irreversible and reversible contributions. Here, we are interested in the irreversible contributions which are related to the current "frozen" domain state at a given instant of the loading history. Such irreversible contributions are obtained by a so-called "fictitious" unloading process. The corresponding reversible contributions are calculated by means of fixed dielectric, piezoelectric and elastic constants determined for the given instant of the loading or unloading curve by the partial unloading method. The above approach has to be distinguished from "real" complete unloading during which the domain state is changed due to back-switching.[13] In view of the above discussion, we calculate the irreversible longitudinal and transverse strains as well as the polarization in using the equations

$$S_3^{ir} = S_3 - S_3^{rev} = S_3 - d_{33}E_3, \tag{4}$$

$$S_1^{ir} = S_1 - S_1^{rev} = S_1 - d_{31}E_3, \tag{5}$$

$$P_3^{ir} = P_3 - P_3^{rev} = P_3 - \varepsilon_{33}E_3. \tag{6}$$

Here, S_3, S_3^{rev} and S_3^{ir} are the actual total strains, reversible strains and irreversible strains in axial direction, while S_1, S_1^{rev} and S_1^{ir} are the actual total strains, reversible strain and irreversible strain in transverse direction. P_3, P_3^{rev} and P_3^{ir} are the total, reversible and irreversible polarization. d_{33} and d_{31} denote the current piezoelectric constants in axial and transverse directions, and ε_{33} is the dielectric constant, which belong to a domain state "frozen" at the considered instant of the loading history as they are obtained by fast partial unloading cycles.

The results calculated for the strains in longitudinal and transverse directions and for the polarization during both loading and unloading are shown in Fig. 5. The total, reversible and irreversible strain curves all show a clear "butterfly" hysteresis loop trend.

For specimens in the initially unpoled state, no macroscopic polarization and strain can be observed in the region of $E_3 < 0.34$ kV/mm. This is because the electric field is much lower than the so-called coercive field E_c strength and, therefore, domain switching cannot be initiated. The total, reversible, and irreversible strain curves almost overlap and the magnitudes of polarization and strains are nearly equal to zero. With the electric field in the neighborhood of E_c, the domains are gradually aligned to the loading direction. A fast development of both polarization and strains can be observed. For strain–electric field loops, the significant increase in total strain is due to two different contributions. First, the irreversible part results from the increasing number of domains reoriented with their polar axes parallel to the electric field. Second, the reversible part is due to the inverse piezoelectric effect originating from the gradually increasing piezoelectric constant. For the polarization–electric field loops, due to internal stresses after poling some unstable domains switch back to their position in the initially unpoled state. Most of the domains, however, may be considered to stay aligned parallel to the poling direction. Hence, the irreversible hysteresis curve is much more pronounced than the reversible one.

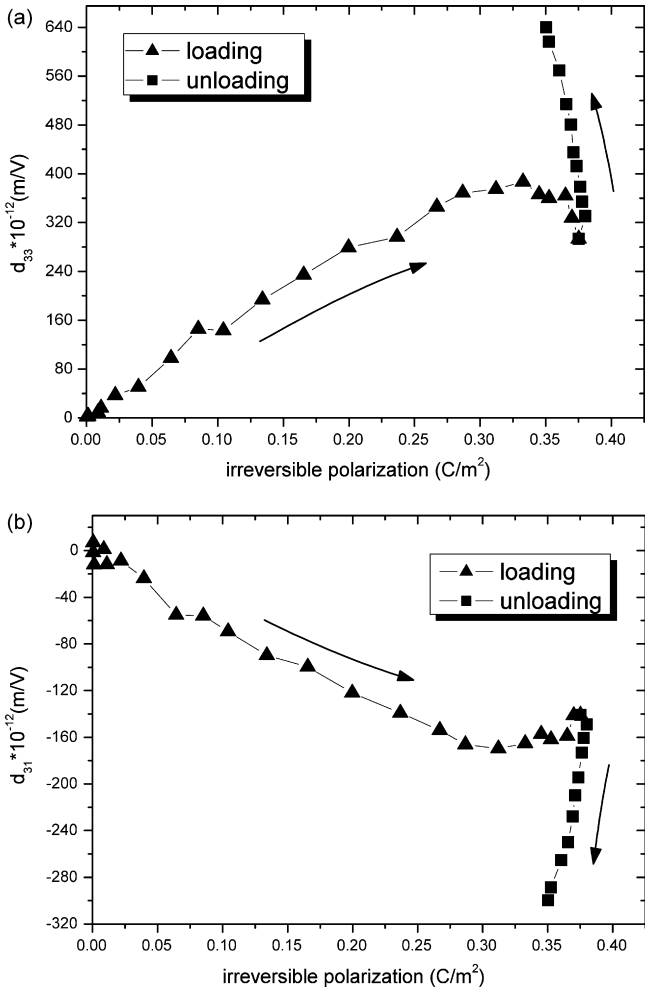

Fig. 6. Piezoelectric constants during loading and unloading processes in axial direction (a) and transverse direction (b) plotted vs. irreversible polarization.

3.1.3. Piezoelectric coefficients and irreversible strains as functions of irreversible polarization

As shown in Fig. 6(a) and (b), both d_{33} and d_{31} seem to be reasonably linear functions of irreversible polarization during

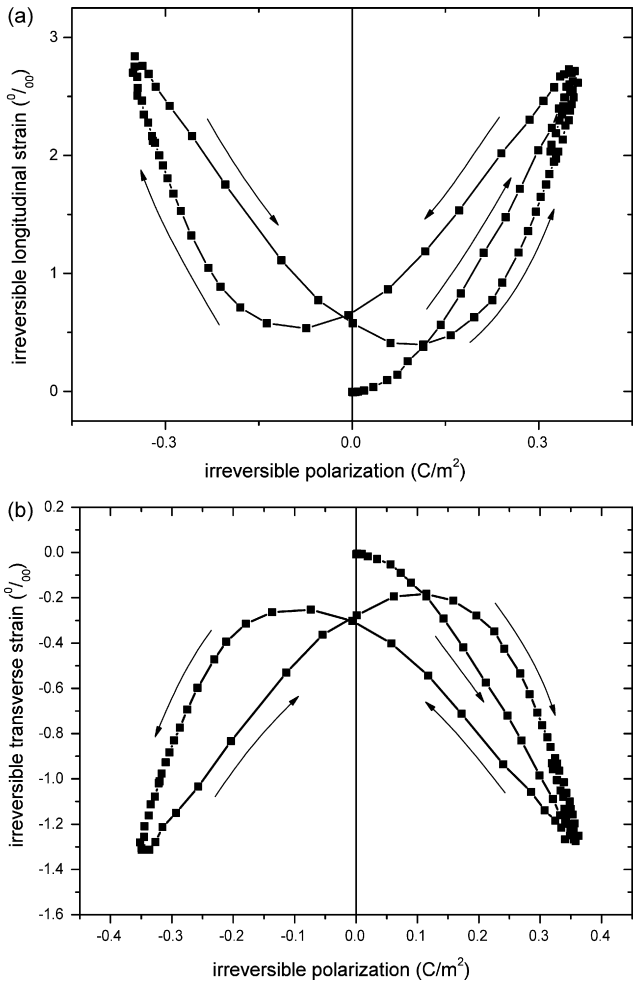

Fig. 7. Evolution of irreversible strains in axial and transverse directions plotted vs. irreversible polarization.

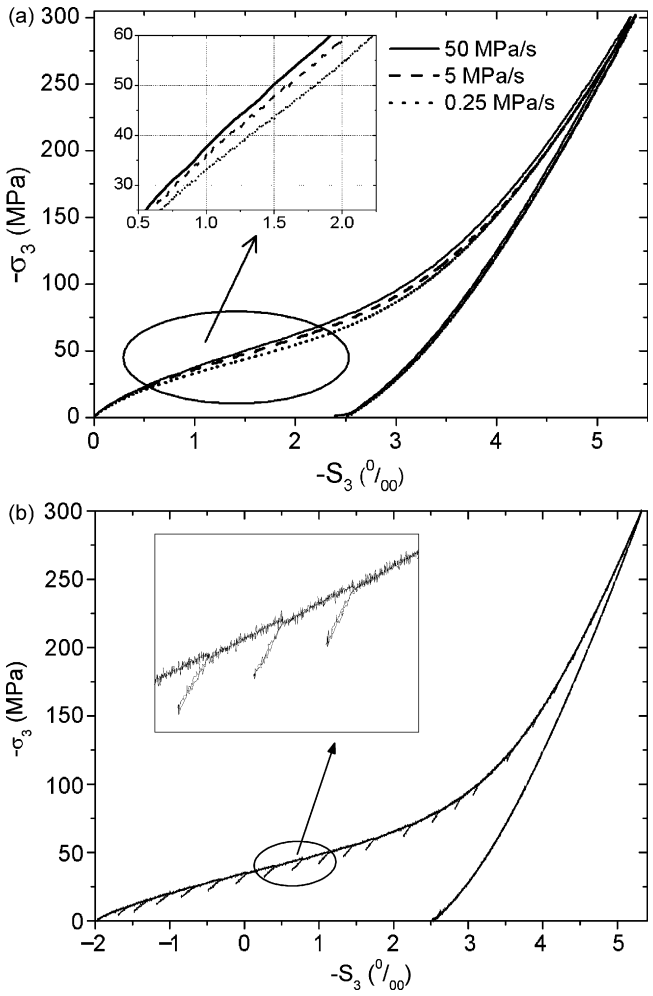

Fig. 8. (a) Uniaxial stress–strain curves of an initially unpoled soft PZT measured at different loading rates of 50, 5, and 0.25 MPa/s and (b) stress–strain curve measured using the partial unloading method.

the loading and unloading process, however, the slopes are different. Besides these general trends, there are some interesting details. First of all, during loading both piezoelectric coefficients pass through a maximum value and show a trend to decrease again close to the maximum irreversible polarization. Second, both coefficients increase further as irreversible polarization is reduced during unloading the electric field. We would attribute both findings to the fact that the high electric fields leading to high irreversible polarization values reduce domain wall mobility thus inhibiting the extrinsic contribution to the piezoelectric effect coming from reversible domain wall motion. Thus, the piezoelectric coefficients are not simply linear functions of irreversible polarization.

Fig. 7 shows the evolution of irreversible polarization and irreversible strains in (a) axial and (b) transverse directions. During a full cycle of the electric field, the longitudinal irreversible strain over irreversible polarization appears to follow a "butterfly" relation, while the transverse irreversible strain over irreversible polarization follows an "inverse butterfly" relation. The curves in irreversible polarization and irreversible strains space are nearly symmetric about the irreversible strain axis. The general trend of the hystereses resembles an electrostrictive-type of quadratic parabola. Obviously, irreversible strain is not simply a function of irreversible polarization and consequently irreversible polarization and strain will have to be used both together as internal variables to describe the material behaviour as functions of loading and unloading history in constitutive modeling.

3.2. Pre-poled soft PZT under compressive stress loading

3.2.1. Elastic and piezoelectric coefficients

Fig. 8(a) shows the axial stress–strain curves measured for initially unpoled soft PZT under continuous compression load with different loading rates.[25] As illustrated in the inserted figure, the strain response of ferroelectrics depends strongly on the loading rate, especially in the non-linear region. At the same stress level, the general evolution follows the principle that the lower the loading rate, the higher the amount of induced strain. It has been proven that piezoceramics exhibit a primary or transient type of creep behavior as the external loads applied are kept constant for extended periods of time.[26] It is presumable that, when an infinitely slow loading rate is used, a final stable irreversible strain state will be induced at each stress amplitude.

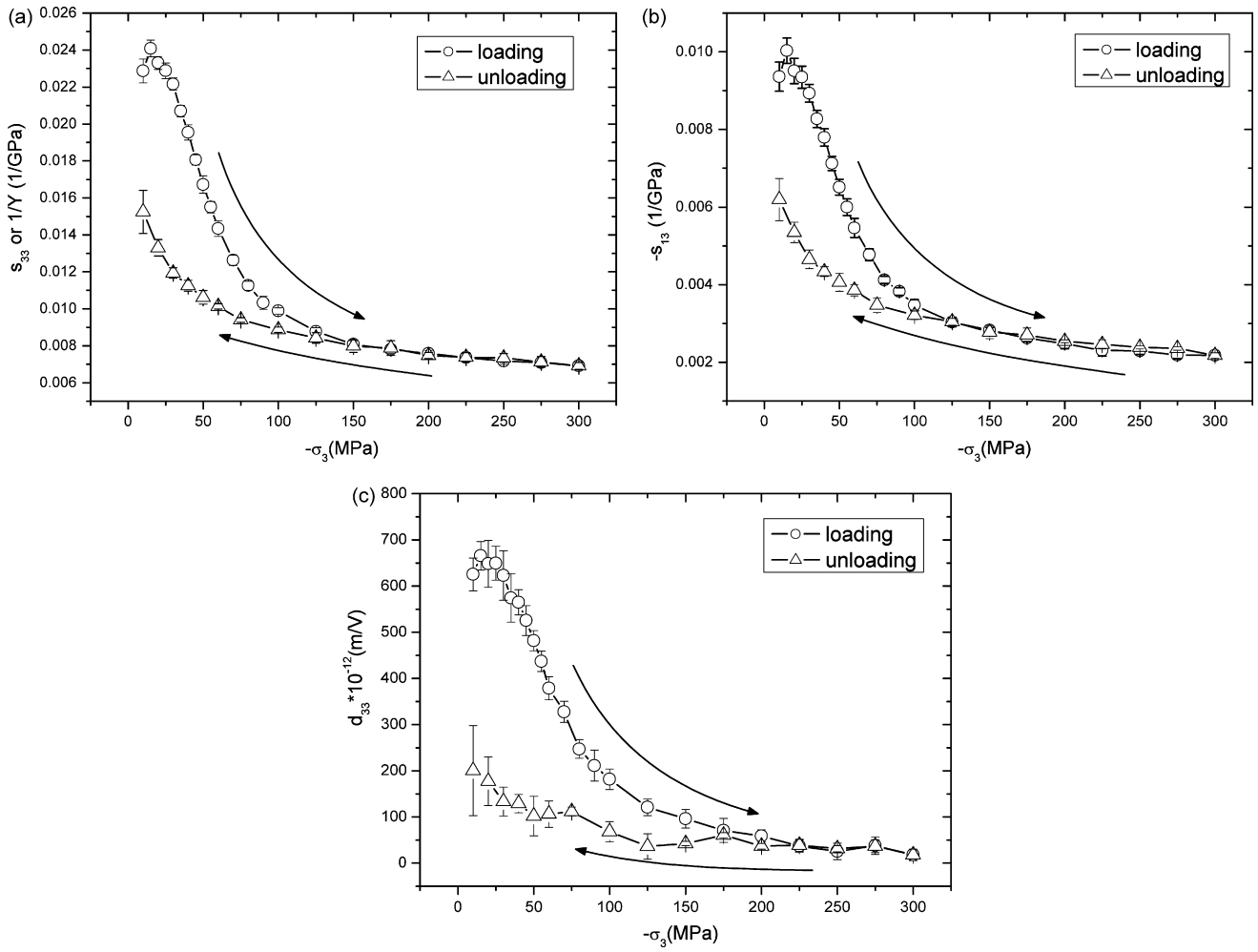

Fig. 9. Elastic compliances in axial (a) and transverse (b) directions and piezoelectric constant (c) in axial direction plotted vs. compressive stress for soft PZT in the pre-poled state.

Time-dependent effects of piezoceramics have to be minimized in an investigation of the loading history dependence of the linear parameters.[18] Therefore, when using the partial unloading method, the desired loading conditions are: (1) the main stress should be applied as slow as possible; (2) the magnitude ($\Delta\sigma_3$) and the duration (Δt) of the partial unloading should be as small as possible.

Fig. 8(b) presents the curve of axial strain versus compressive stress as measured using the partial unloading method. As described in Section 2, the loading rate of the applied main stress is very slow ($\dot{\sigma}_3 = 0.25$ MPa/s). At a certain pre-determined level of the main stress, the specimen is exposed to a pulse-shaped partial unloading with $\Delta\sigma_3 \approx 10$ MPa and $\dot{\sigma}_3 = 5$ MPa/s. In this way, it was taken care to reduce the influence of time-dependent effects as much as possible.

As shown in the inset of Fig. 8(b), the strain–stress curves during partial unloading could be fitted well as straight lines. The material parameters at different main stress levels can be obtained from the slopes of the fitting,

$$\frac{1}{s_{33}} = Y = \frac{\Delta\sigma_3}{\Delta S_3}, \tag{7}$$

$$\frac{1}{s_{13}} = \frac{\Delta\sigma_3}{\Delta S_1}, \tag{8}$$

$$d_{33} = \frac{\Delta P_3}{\Delta\sigma_3}. \tag{9}$$

Here, $\Delta\sigma_3$ is the magnitude of the partial unloading stress, ΔS_3 and ΔS_1 stand for the changes of longitudinal and transverse strains, respectively, s_{33} and s_{13} indicate the elastic compliances, Y is the Young's modulus, and ΔP_3 and d_{33} represent the change of polarization and the piezoelectric constant, respectively.

Poisson's ratio (ν) determined during partial unloading is given by

$$\nu = -\frac{\Delta S_1}{\Delta S_3} = -\frac{s_{13}}{s_{33}}. \tag{10}$$

In Fig. 9 the elastic compliances measured in axial and transverse directions and the piezoelectric constant are plotted versus the main stress values at which partial unloading was performed. For the pre-poled PZT in an initially stress-free state, elastic compliances s_{33} and $-s_{13}$ of about 0.023 GPa^{-1} and 0.009 GPa^{-1}, respectively, are obtained. The value for s_{33} is comparable to 0.019 GPa^{-1} given by the manufacturer PI

Ceramic. The compliances s_{33} and s_{13} as well as the piezoelectric coefficient d_{33} exhibit a non-linear behavior with an initial moderate increase followed by a significant decrease at high stress magnitudes. Both intrinsic and extrinsic contributions are included to the elastic and piezoelectric responses. The extrinsic contributions due to reversible domain wall motion are more important in soft PZT.[20,21] As shown in Fig. 9, the initial increases in s_{33}, s_{13}, and d_{33} are caused by additional extrinsic contributions at low stresses. As the stress magnitude is increased further, the decreasing of the compliances and the piezoelectric coefficient can be attributed to an increasing amount of domains reoriented perpendicular to the stress loading direction by stress induced ferroelastic domain switching. In this experiment, non-180° domain switching is initiated at stresses as low as about 20 MPa and is completed at ~150 MPa. In the stress region between 150 MPa and 300 MPa, the elastic compliances produced in stress loading and unloading basically follow an almost straight line. At 300 MPa, s_{33} and s_{13} reach their lowest values, which means that the PZT material is stiffened by the compressive stress. When unloading the compression load below 150 MPa, the elastic compliances and the piezoelectric coefficient increase non-linearly. At the end of a cycle, the s_{33} and s_{13} values are much lower than their initial values. It is understood that unit cells and domains are less compliant in the direction perpendicular to their polar axis. Consequently non-180° domain switching under compressive stresses leads to stiffer behavior in the direction of loading.[17] This is in complete agreement with our measurements. The hysteresis-free decrease of the compliances in the range between 150 MPa and 300 MPa is caused by the increasing constraint to reversible domain wall mobility due to the presence of very high main stresses.

As shown in Fig. 9(c), the piezoelectric coefficient is reduced to a minimum after the stress reaches 175 MPa, which means that very little piezoelectric activity is left. As the stress is unloaded from 300 MPa to 0 MPa, d_{33} recovers partially. The value of d_{33} at zero stress is tremendously lower than the initial one, which indicates that depoling induced by the compressive stress was highly effective. Less than 20% of the original piezoelectric effect remains after mechanical depolarization.

Fig. 10 displays the dependence of Young's modulus (a) and Poisson's ratio (b) of initially pre-poled soft PZT on compressive stress at zero external electric field. In the region of $0 \leq -\sigma_3 \leq 100$ MPa, Young's modulus exhibits a strong variation from 44 GPa to 101.2 GPa. At the beginning of the loading process $\sigma_3 = 0$ MPa, Young's modulus is about 44 GPa. At 300 MPa, a maximum value of Young's modulus of $Y \approx 140$ GPa is reached. During the unloading, Young's modulus initially decreases along the loading paths. At stresses below 150 MPa, the values are higher than those measured during the loading process. Of course, all these observations are related straightforwardly to the discussion of the compliances.

Due to the limited resolution of the measurement systems and the noises of the signals, the values of Poisson's ratio scatter somewhat, but the trend is clear. Starting from $\nu \approx 0.41$, the Poisson's ratio decreases non-linearly with increasing load and approaches the value of 0.32 at 300 MPa. During the unloading process, the Poisson's ratio increases non-linearly and slightly

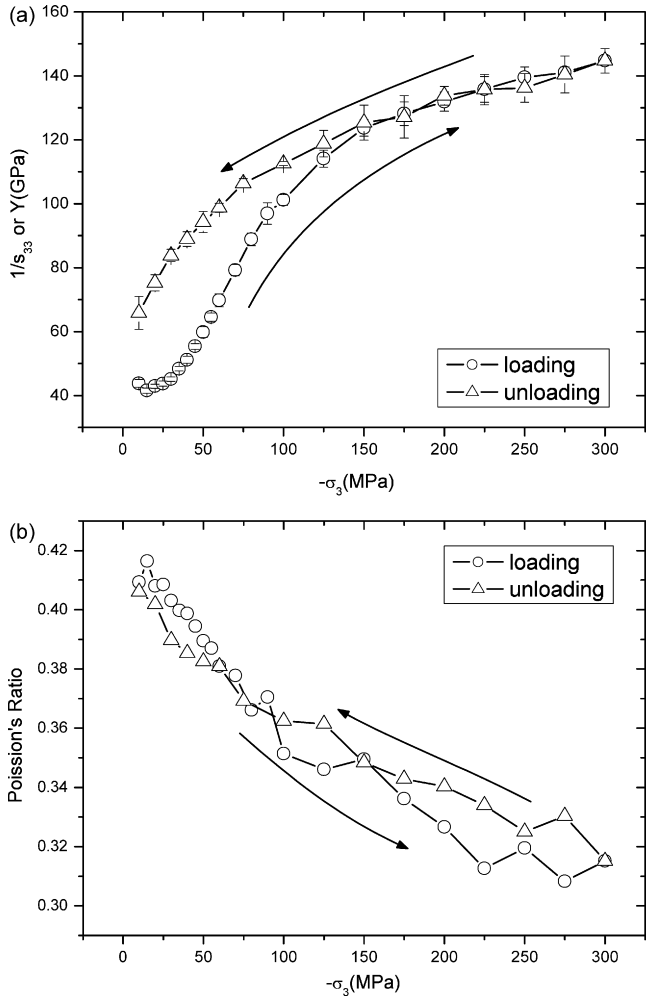

Fig. 10. Young's modulus (a) and Poisson's ratio (b) plotted vs. compressive stress for soft PZT in the pre-poled state.

exceeds the values at the same stress level in the loading process before the stress is reduced to 100 MPa. After this, Poisson's ratio is lower than that in the loading process.

3.2.2. *Separation of reversible and irreversible strains and polarization*

The measurement of material parameters at variable stress levels allows for a separation of reversible and irreversible contributions. The irreversible strains in axial and transverse directions and irreversible axial polarization due to domain switching are calculated using the following equations:

$$S_3^{ir} = S_3 - S_3^{rev} = S_3 - s_{33}\sigma_3, \tag{11}$$

$$S_1^{ir} = S_1 - S_1^{rev} = S_1 - s_{13}\sigma_3, \tag{12}$$

$$P_3^{ir} = P_3 - P_3^{rev} = P_3 - d_{33}\sigma_3. \tag{13}$$

Here, S_3, S_1, S_3^{rev}, S_1^{rev} and S_3^{ir}, S_1^{ir} are the total, reversible, and irreversible strains in axial and transverse directions, respectively. P_3, P_3^{rev} and P_3^{ir} represent the total, reversible and irreversible polarization. s_{33}, s_{13}, and d_{33} denote the compliances in axial and transverse directions, respectively, and the piezoelectric coefficient.

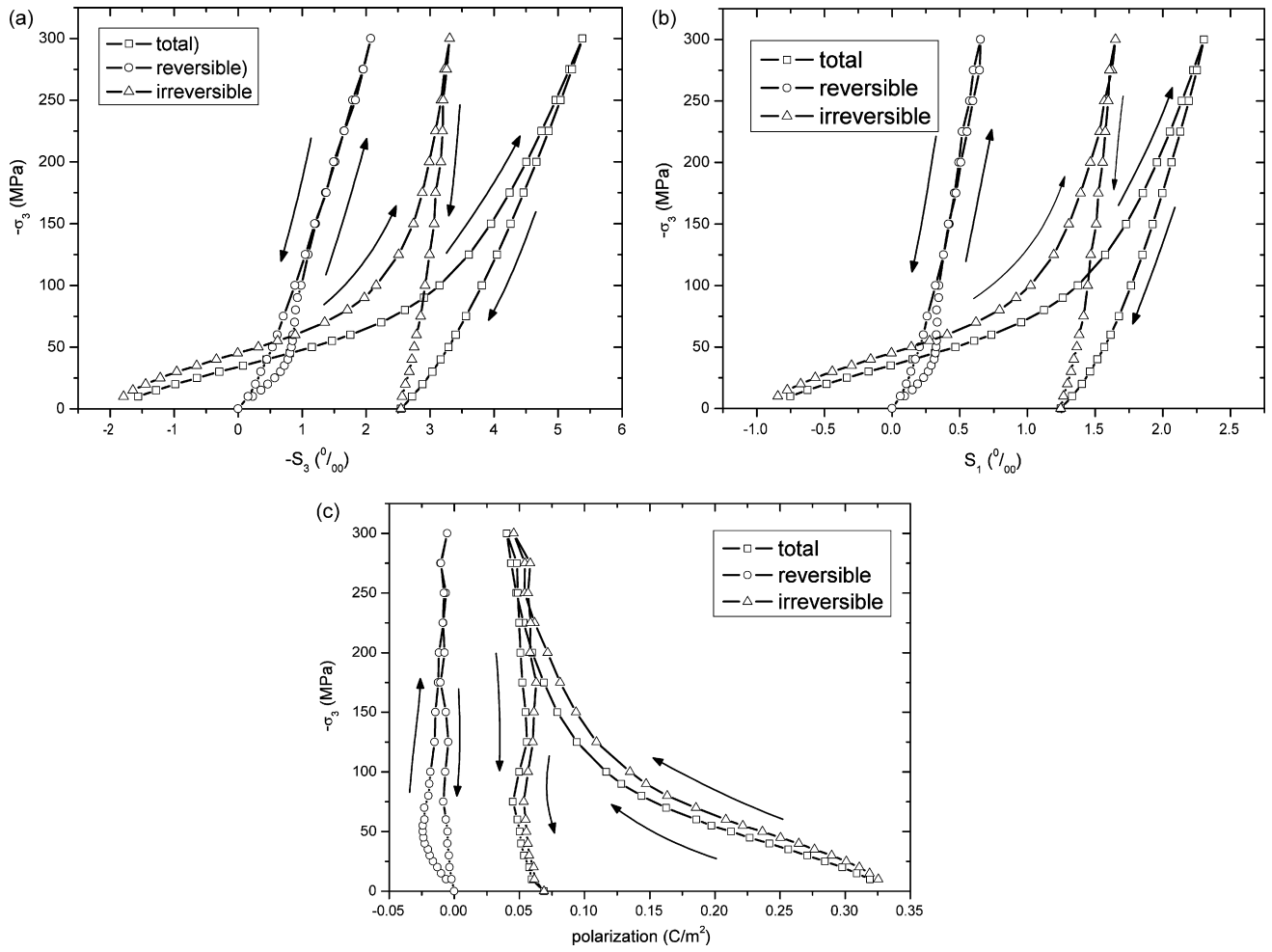

Fig. 11. Total, reversible and irreversible strains in longitudinal (a) and transverse (b) directions and polarization (c) in axial direction.

The calculated results for the strains in longitudinal (a) and transverse (b) directions and axial polarization (c) during the loading and unloading processes are shown in Fig. 11. In the region of $-\sigma_3 < 100$ MPa the strains and polarization responses are clearly non-linear and irreversible parts of strains and polarization are induced. After this, the increments of the irreversible parts get smaller and these tend to be saturated. During the unloading process, the irreversible parts are not constant, but decrease only slightly in a non-linear manner due to partial back-switching of domains initiated by the internal stresses and fields. Looking at the reversible parts, the behavior for stresses $-\sigma_3 < 50$ MPa in the loading branch is quite interesting. It can clearly be seen that the material is much softer in the mechanical and dielectric sense in this region. This has to be attributed to strong extrinsic contributions by reversible domain wall motion. As the stresses are increased, domain wall mobility is more and more constrained and mainly the intrinsic contribution to the reversible quantities is left. Interestingly, no significant extrinsic contributions are visible close to the complete unloading after having reached a completely switched domain structure at very high stresses. After complete unloading of the compressive stress, the reversible parts of polarization and strains return to zero.

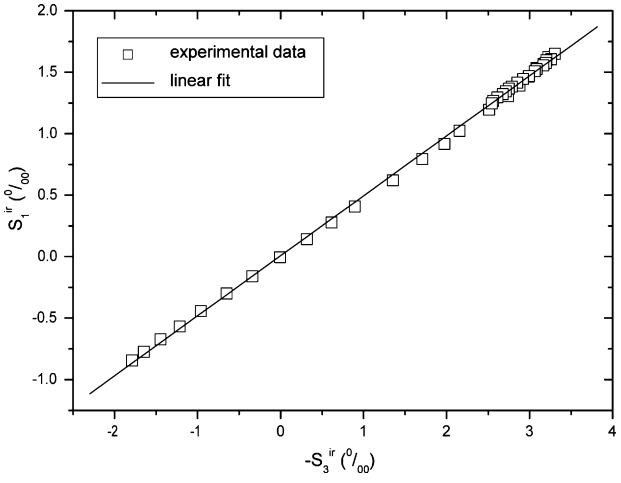

Fig. 12. Correlation between irreversible strains in axial and transverse directions.

3.2.3. Discussion of irreversible volumetric strain

The PIC151 soft PZT material used in these tests has a composition near the morphotropic phase boundary (MPB) with a coexistence of tetragonal and rhombohedral phases. Uniaxial electric field or mechanical stress loading may induce a phase

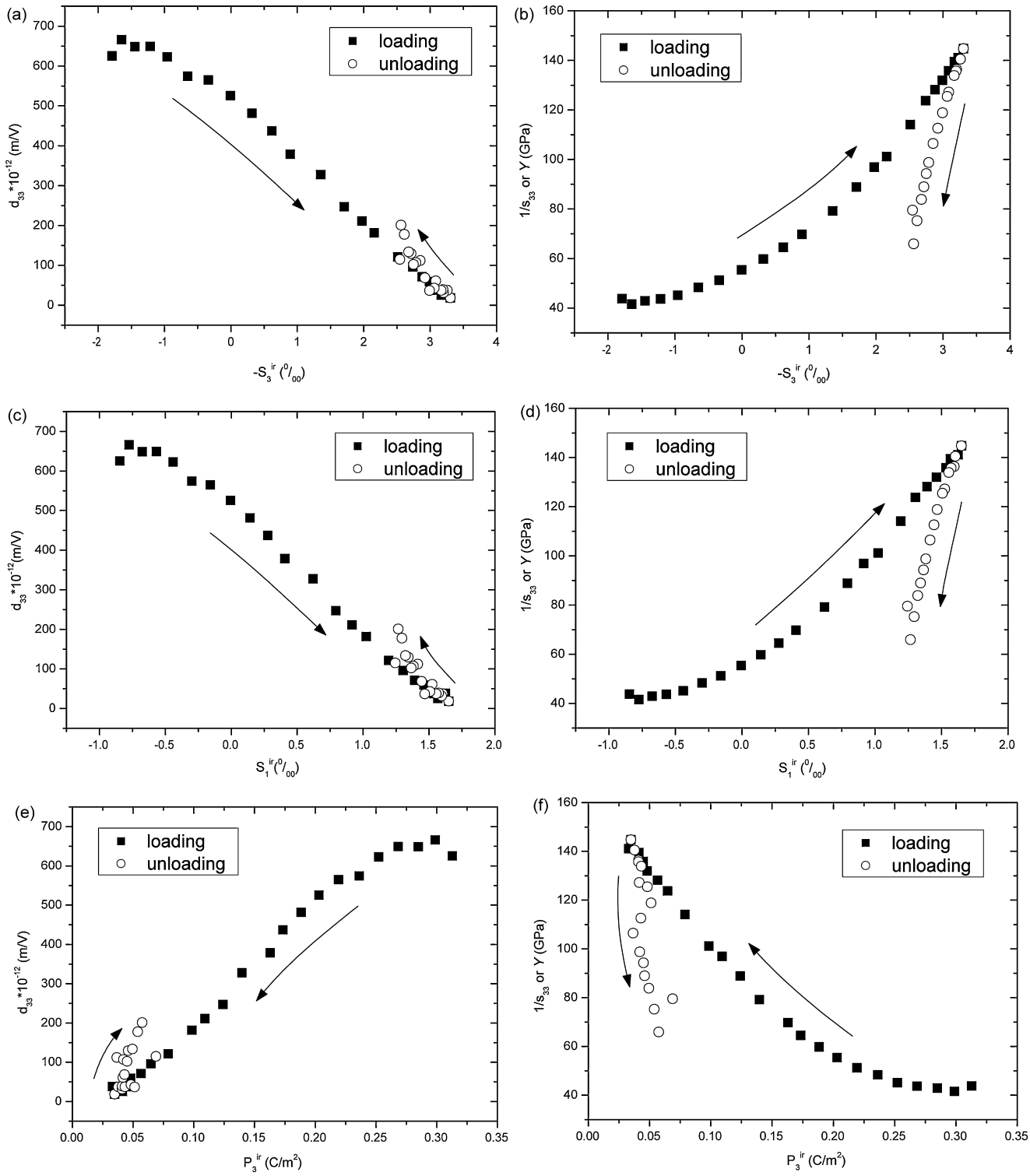

Fig. 13. Piezoelectric constant in axial direction and Young's modulus plotted vs. irreversible axial strain ((a) and (b)), irreversible transverse strain ((c) and (d)) and irreversible polarization ((e) and (f)).

transition as indicated by calculations based on thermodynamic theory.[27] We expect, in the former case, the transition to be from the rhombohedral phase to the tetragonal phase while, in the latter case, to be the other way around. Microstructural analyses have shown that the unit cell volume of the tetragonal phase (67.8833 Å^3) is larger than that of the rhombohedral phase (67.5667 Å^3).[28]

Since the tests are carried out under uniaxial compressive stress loading, the transverse deformation is isotropic, yielding $S_1 = S_2$. Hence, the relative change of the material's volumetric strain (S_{volume}) resulting from plastic deformation due to ferroelastic domain switching can be expressed as

$$S_3^{ir} + 2S_1^{ir} = S_{\text{volume}}. \tag{14}$$

It is understood that no volume change occurs during pure domain switching. Therefore, if the irreversible strains are caused by domain switching alone, one obtains $S_{\text{volume}} = S_3^{ir} + 2S_1^{ir} = 0$. As a result, the ratio of S_1^{ir} to S_3^{ir} is expected to be 0.5.

For pre-poled PZT, Fig. 12 shows the plot of measured irreversible transverse strain versus irreversible axial strain. The experimental data can be fitted well by a straight line. The slope of this linear fit is about 0.488, which is slightly lower than the value of 0.5 expected for pure domain switching processes. The result indicates that a negative irreversible volumetric strain ($S_{\text{volume}} < 0$) was induced in the pre-poled PZT material under compressive stress loading.

For the strain data obtained under electric field loading reported in Section 3.2.1, the same evaluation with respect to the volumetric strain evolution has been carried out. In this case, a value of 0.469 was obtained for the slope of $-S_1^{ir}$ plotted versus S_3^{ir}, i.e. for the ratio $-S_1^{ir}/S_3^{ir}$. This means an increase of volumetric strain during electric field loading ($S_{\text{volume}} > 0$), and the effect is even slightly stronger than in the case of compressive stress loading.

In summary, for the reasons mentioned above, we suggest an explanation of the observed changes in volumetric strain to be due to the occurrence of load induced phase transitions of small fractions of the material. In the case of compressive stress loading, we have a transition from the tetragonal phase to the rhombohedral phase while there is a transition from the rhombohedral phase to the tetragonal phase for electric field loading starting from the unpoled state.

3.2.4. Correlations of irreversible parameters

The measurement conditions have a significant impact on the response of the piezoelectric material, such as the loading rate effects shown in Fig. 8. On the other hand, in control theory, for instance, the material properties are conventionally described as functions of mechanical stress and electric field. From a principle point of view, such an approach is not sufficient to describe the loading history dependence of the material coefficients of ferroelectrics. Rather, for purposes of constitutive modeling, it is important to describe the material tensors in dependence on appropriately chosen state variables (internal variable, memory variable). In this sense, the measured piezoelectric constants and Young's modulus are plotted versus irreversible strain and irreversible polarization, respectively, in Fig. 13. It is obviously seen in Fig. 13(b), (d), and (f) that Young's modulus follows different paths during loading and unloading if plotted versus irreversible strains and polarization. This indicates that the loading history dependence of the elasticity constants cannot simply be described by irreversible strain or irreversible polarization, respectively, as the only internal variable. This effect seems not to be so pronounced in the plots of the piezoelectric constant in Fig. 13(a), (c), and (e), however, a deviation between loading and unloading paths is present in all these plots as well.

As shown in Fig. 14, both longitudinal irreversible strain and transverse irreversible strain seem to be reasonably linear functions of irreversible polarization. However, such a simple linear correlations was not observed in Fig. 9. There, both 180° and non-180° domain switching induced by bipolar electric field loading gives rise to non-linear hysteresis loops of S^{ir} versus P^{ir}. In Fig. 14, we deal with a unipolar mechanical loading–unloading cycle, where only non-180° domain switching is involved.

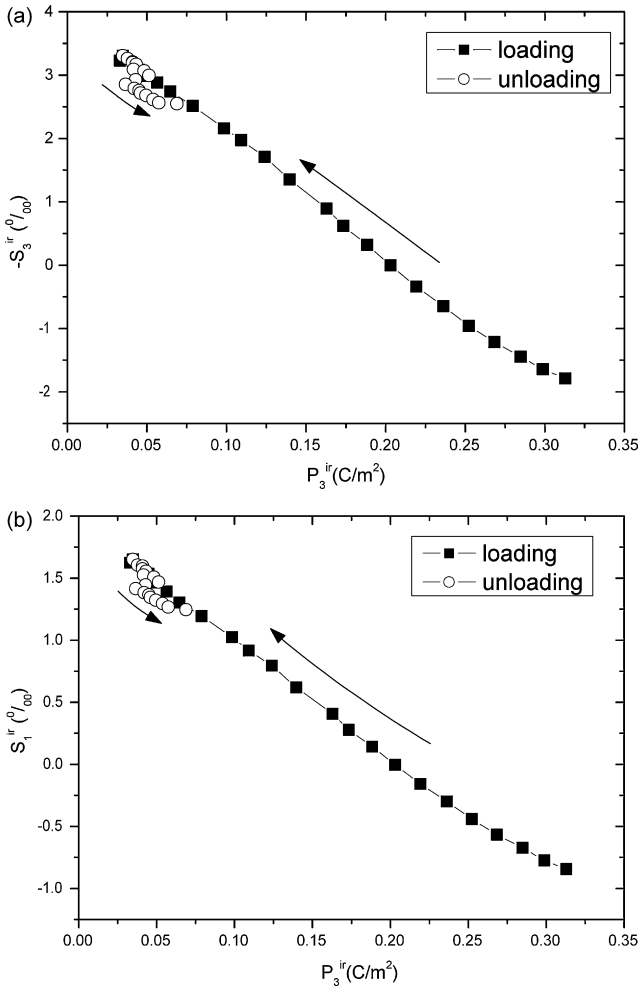

Fig. 14. Evolution of irreversible strains in axial and transverse directions plotted vs. irreversible polarization.

In summary, to represent the material properties accurately, it is not sufficient to introduce irreversible strain or irreversible polarization alone as the only internal variable to describe the history dependence of material tensors in constitutive modeling.

4. Conclusions

In the current experimental study, fast small-electric-field and small-stress partial unloading methods were used to measure the material properties of initially unpoled soft PZT under pure electric field (A) and of initially pre-poled soft PZT under compressive stress loading (B). In experiment (A), piezoelectric coefficients and dielectric permittivity were evaluated as function of the electric field. It was found that the piezoelectric constant and dielectric permittivity depend on the electric field history. Interestingly, the piezoelectric coefficients were found to decrease after having reached peak levels. The plots of the piezoelectric coefficient plotted versus irreversible polarization

deviated significantly from each other during the loading and unloading processes. Irreversible polarization and irreversible strains showed a "butterfly" hysteresis correlation and were nearly symmetric about the irreversible polarization axis. As a consequence, both irreversible polarization and irreversible strain may have to be used as internal variables for describing the loading and unloading history of material properties in constitutive modeling. The obtained material coefficients were used to separate reversible strain and reversible polarization from the corresponding irreversible quantities which are caused by domain switching.

In experiment (B), the strain response was found to depend significantly on the loading rate confirming the need for fast partial unloading cycles. Elastic moduli and piezoelectric coefficient were evaluated as a function of compressive stress. Both turned out to be dependent on the stress history. The results were used to separate the reversible strain and polarization from the irreversible ones due to domain switching. Furthermore, the correlation between irreversible strains in transverse and axial directions was studied, and the ratio is slightly lower than the value of 0.5, which would indicate pure volume preserving domain switching. The result indicates that a negative irreversible volumetric strain ($S_{\text{volume}} < 0$) has been induced. The measured piezoelectric constant and Young's modulus were plotted versus longitudinal irreversible strain and irreversible polarization. A deviation of trends was observed during loading and unloading processes. Both longitudinal irreversible strain and transverse irreversible strain seemed to be reasonably linear with respect to irreversible polarization. To represent the material properties more accurately, it was therefore deduced to be necessary to introduce irreversible strains and irreversible polarization as internal variables to describe the material behaviour in constitutive modeling.

Acknowledgement

Financial support of this work by the Deutsche Forschungsgemeinschaft (DFG) under grant ZH 62/1-2 is gratefully acknowledged.

References

1. Akhras G. Smart materials and smart systems for the future. *Can Mil J* 2000;**Autumn**:25–32.
2. Uchino K. *Ferroelectric devices*. New York: Marcel Dekker; 2000.
3. Haertling GH. Ferroelectric ceramics: history and technology. *J Am Ceram Soc* 1999;**82**(4):797–818.
4. Mueller-Fiedler R, Knoblauch V. Reliability aspects of microsensors and micromechatronic actuators for automotive applications. *Microelectron Reliab* 2003;**43**:1085–97.
5. Zhou D. Experimental investigation of non-linear constitutive behavior of PZT piezoceramics. PhD Thesis. University of Karlsruhe (TH); 2003 [published as research report of Forschungszentrum Karlsruhe, FZKA 6869].
6. Jaffe B, Cook Jr WR, Jaffe H. *Piezoelectric ceramics*. New York: Academic Press; 1971.
7. Xu Y. *Ferroelectric materials and their applications*. Amsterdam: North-Holland; 1991.
8. Lynch CS. The effect of uniaxial stress on the electro-mechanical response of 8/65/35 PLZT. *Acta Mater* 1996;**44**(10):4137–48.
9. Chaplya PM, Carman GP. Dielectric and piezoelectric response of lead zirconate–lead titanate at high electric and mechanical loads in terms of non-180° domain wall motion. *J Appl Phys* 2001;**90**(10):5278–86.
10. Kamlah M. Ferroelectric and ferroelastic piezoceramics—modeling of electromechanical hysteresis phenomena. *Continuum Mech Thermodyn* 2001;**13**(4):219–68.
11. Landis CM. Non-linear constitutive modeling of ferroelectrics. *Curr Opin Solid State Mater Sci* 2004;**8**:59–69.
12. Zhou D, Kamlah M, Munz D. Effects of uniaxial prestress on the ferroelectric hysteretic response of soft PZT. *J Eur Ceram Soc* 2005;**25**:425–32.
13. Liu QD, Huber JE. State dependent linear moduli in ferroelectrics. *Int J Solid Struct* 2007;**44**:5635–50.
14. Schaeufele AB, Haerdtl KH. Ferroelastic properties of lead zirconate titanate ceramics. *J Am Ceram Soc* 1996;**79**(10):2637–40.
15. Chaplya PM, Carman GP. Compression of piezoelectric ceramic at constant electric field: energy absorption through non-180° domain-wall motion. *J Appl Phys* 2002;**92**(3):1504–10.
16. Zhou D, Kamlah M, Munz D. Effects of bias electric fields on the nonlinear ferroelastic behavior of soft lead zirconate titanate piezoceramics. *J Am Ceram Soc* 2005;**88**(4):867–74.
17. Fett T, Munz D, Thun G. Young's modulus of soft PZT from partial unloading tests. *Ferroelectrics* 2002;**274**:67–81.
18. Selten M, Schneider GA, Knoblauch V, McMeeking RM. On the evolution of the linear material properties of PZT during loading history—an experimental study. *Int J Solid Struct* 2005;**42**:3953–66.
19. Böttger U. Dielectric properties of polar oxides. In: Waser R, Böttger U, Tiedke S, editors. *Polar oxides: properties, characterization, and imaging*. Weinheim: Wiley; 2005. p. 11–38.
20. Zhang QM, Pan WY, Cross LE. Domain wall excitations and their contributions to the weak-signal response of doped lead zirconate titanate ceramics. *J Appl Phys* 1988;**64**:6445.
21. Zhang QM, Wang H, Kim N, Cross LE. Direct evaluation of domain-wall and intrinsic contributions to the dielectric and piezoelectric response and their temperature dependence on lead zirconate–titanate ceramics. *J Appl Phys* 1994;**75**(1):454–9.
22. Damjanovic D. Ferroelectric, dielectric and piezoelectric properties of ferroelectric thin films and ceramics. *Rep Prog Phys* 1998;**61**:1267–324.
23. Press WH, Teukolsky SA, Vetterling WT, Flannery PB. *Numerical recipes in C—the art of scientific computing*. 2nd ed. Cambridge University Press; 1992. p. 703–5.
24. Ogawa T. Domain structure of ferroelectric ceramics. *Ceram Int* 2000;**26**:383–90.
25. Zhou D, Kamlah M, Gan Y, Laskewitz B. Time-dependent non-linear ferroelastic behavior of soft lead zirconate titanate piezoceramics. *Adv Sci Technol* 2006;**45**:2464–71.
26. Zhou D, Kamlah M. Room-temperature creep of soft PZT under static electrical and compressive stress loading. *Acta Mater* 2006;**54**:1389–96.
27. Stotz S. Shift of the morphotropic phase boundary in the PZT system under the influence of electric fields and uniaxial stresses. *Ferroelectrics* 1987;**76**:123–32.
28. Soares MR, Senos AMR, Mantas PQ. Phase coexistence region and dielectric properties of PZT ceramics. *J Eur Ceram Soc* 2000;**20**:321–34.